RSC Advances

PAPER

View Article Online
View Journal | View Issue

Cite this: *RSC Adv.*, 2021, **11**, 13466

Synthesis and properties of organoboron functionalized nanocellulose for crosslinking low polymer fracturing fluid system

Yanling Wang,* Chuanbao Zhang, Ning Xu, Jincheng Lan, Baoyang Jiang and Lingtao Meng

The traditional organoboron crosslinker used in the guar gum fracturing fluid has the disadvantages of a larger amount of guar gum and crosslinker and higher susceptibility to pH. Nanoparticles have special properties such as large specific surface area and many active groups, so the organic boron crosslinker and nanoparticles are combined to obtain nano crosslinkers. In this paper, rod-shaped nano-cellulose particles were prepared by acid hydrolysis, and a nanocellulose crosslinker was synthesized by combining with organic boron and KH550. Nanocellulose cross-linker has good temperature and salt resistance. It can meet the requirements of cross-linking guar gum fracturing fluid with a mass fraction of 0.3 wt% under neutral conditions. The residual viscosity is higher than 50 mPa s under shear at 170 s^{-1} and 110 °C for 60 minutes when the pH increases from 7 to 13, and NBC crosslinking can withstand a temperature of 160 °C under pH = 10. The crosslinking mechanism of the widely accepted nano-crosslinker is that the organoboron on the surface of the nanoparticle combines with the homeopathic *ortho* hydroxyl of the guar gum molecule to form a hydrogen bond and thereby form a complex network structure. This research shows that the hydrogen bonding between the nano-cellulose crosslinker and HPG molecules, and the resulting gel has a more complex network structure because of the formation of inter-chain cross-links.

Received 30th November 2020
Accepted 5th April 2021

DOI: 10.1039/d0ra10105b

rsc.li/rsc-advances

1. Introduction

Hydraulic fracturing is an effective technology to develop low permeability reservoirs. Water-based fracturing fluids are most commonly used because of their excellent properties such as strong ability to suspend sand, low fluid loss, and low friction.[1,2] Guar gum and its derivatives have been used as thickeners for decades.[3,4] Guar gum is a naturally occurring galactomannan, which consists of linear chains of (1→4)-β-D-mannopyranosyl units with α-D-galactopyranosyl units attached by a (1→6) linkage.[5] In order to higher solubility and temperature stability, native guar gum is often derivatized with propylene oxide resulting in hydroxypropyl guar gum (HPG). When guar is modified to HPG, the added hydroxypropyl groups sterically block the hydrogen bonding sites on the guar backbone and reduce the hydrogen bonding attractions between guar molecules. Therefore, HPG molecules will be fully extended in water, the dispersibility in water will be improved, and the viscosity-increasing effect of the solvent will become better.[6,7] Gelling of the fracturing fluid is formed by combining crosslinker included boric acid, borates, and boron derivatives and zirconium and titanium complexes with thickeners.[8,9] In order to control the crosslinking time and minimize the residue of fracturing fluid, organic boron is usually selected as the cross-linker of guar gum fracturing fluid.[10,11] However, boron compounds cross-link guar only at alkaline pH (>9.5), and the cross-linking process needs to use a larger amount of organoboron and thickener to meet the construction requirements. In addition temperature stability of the gel is limited to 150 °C at the most.[12] The cross-linking mechanism of boron compounds is using hydrolysis to $B(OH)_4^-$ anions generated by hydrolysis form hydrogen bonds with the 3,4-*cis*-hydroxy functionality present in the galactose side chains of guar gum to form the 3D network.[13,14] However, there are fewer cross-linking sites due to the small size of the cross-linker, resulting in a poor cross-linking effect.

Nanoparticles are emerging materials in recent years and are widely used due to their unique properties such as the surface of some nanoparticles is rich in active groups. Surface modification of nanoparticles can form nano-functional compounds.[15] For example, using a silane coupling agent to modify the surface of nanoparticles, and then combining an organoboron cross-linker to obtain nano boron crosslinker, which can increase the size of the crosslinker and the number of crosslinking sites, thereby improving the crosslinking performance. It can achieve for cross-linking at low polymer mass fractions by greatly reducing the amount of guar gum, thereby reducing the cost of fracturing. However, the currently studied nano-crosslinker

College of Petroleum Engineering, China University of Petroleum (East China), Qingdao, 266580, China. E-mail: wangyl@upc.edu.cn

have poor crosslinking effects under neutral conditions and still have a strong dependence on the pH of the base fluid.[16,17] In the known research, most of the nano-crosslinkers are prepared based on surface modification of nano-silicon. Then, it is combined with thickeners such as guar gum and its derivatives, cellulose polymers, and synthetic acrylamide polymers to form a gel with a certain viscosity. Besides, researchers have invented new types of gels such as supramolecular gels, thermo-responsive gels, wormlike micelles. The construction of supramolecular gels system is based on the further multi-level self-assembly of some linear nanostructures to form a three-dimensional network structure, whose mechanical properties are weaker than polymer gels.[18] Thermally responsive gels have a wide range of applications in tissue engineering, drug delivery, and flexible devices.[19] After the worm-like micelle grows to a certain extent, it has high viscosity and viscoelasticity. The molecular weight of the aggregate changes with the change of conditions, so its rheology, relaxation characteristics are different compare with chain polymers.[20,21]

Nanocellulose is a natural nanomaterial which nanometer size in diameter, nanocellulose consists of attractive properties such as high strength, excellent stiffness, and high surface area. The preparation of nanocellulose has a wide range of raw materials and relatively complete preparation technology, which is conducive to its large-scale application. In addition, with its structure, nanocellulose contains a plentiful of hydroxyl groups which are accessible for surface modification.[22,23] Cellulose is composed of repeating β-D-glucopyranose units with three hydroxyl groups per anhydroglucose unit (AGU) providing the cellulose molecule with a high degree of functionality. The versatile application of many are attributed to its properties of biodegradability, biocompatibility, non-toxicity, high functionality, flexibility and high mechanical strength. Nanocrystalline cellulose (NCC) not only possesses inherent features of natural cellulose but also exhibits attractive properties such as high crystallinity index (N70%), large surface area (~150 m^2 g^{-1}), big aspect ratio (~70), high tensile strength, high –OH polar groups which increases surface reactivity, light weight which reduces their density and small particle sizes of range < 500 nm attributing to the increasing interest of the material in recent years.[24] Several techniques have been adopted for the preparation of NCC which includes; high pressure homogenization, high ultra-sonication, acid/alkaline hydrolysis and enzyme assisted hydrolysis as well as the combined processes.[25–27] Among these techniques, acid hydrolysis by sulfuric acid (H_2SO_4) has been commonly used for NCC extraction due to its moderate operation conditions. The NCC suspension prepared by sulfuric acid hydrolysis has good electrostatical stability due to the presence of negative charges.[28,29]

In this study, nano-microcrystalline cellulose was prepared by sulfuric acid hydrolysis, and amino group was grafted onto the surface of nano-microcrystalline cellulose by silane coupling agent KH550.[30] Then, the nano-crosslinker for guar gum fracturing fluid was prepared by *in situ* polymerization method which introduce organic boron onto the surface of reactive nanocrystalline cellulose containing $–NH_2$ group while the reactive nanocrystalline cellulose acts as a carrier.[31] This research reports the performance of the prepared nanocellulose crosslinker in a low polymer fracturing fluid system such as the crosslinking time, the temperature resistance, the durability with salinity and rheological properties of the formed gel. The test results show that the nanocellulose crosslinker has higher crosslinking efficiency and can form a guar gum fracturing fluid gel with better temperature and shear resistance in the pH range of 7–11. In addition, the paper explains the cross-linking mechanism of nanocellulose and guar gum molecules, which provides a basis for subsequent experimental research.

2. Experimental

2.1. Materials

Microcrystalline cellulose, anhydrous ethanol, and gluconic acid sodium salt were purchased from Aladdin Industrial Corporation. Borax, glycerol, and sodium hydroxide were obtained from Chengdu XiYa Chemical Technology Co., Ltd. Sulfuric acid, KCl, and KH550 were supplied by Xilong Scientific Co., Ltd. Hydroxypropyl guar was provided by Sheng Li Oilfield. Deionized water made in the laboratory.

2.2. Synthesis of nanocrystalline cellulose (NCC)

Nanocrystalline cellulose (NCC) was prepared by acid hydrolysis of microcrystalline cellulose (MCC). Diluting 98 wt% concentrated sulfuric acid with deionized water to obtain 65 wt% sulfuric acid solution then adding MCC and 65 wt% sulfuric acid solution to the flask at a ratio of 1 : 8.75 g ml^{-1}, and placing the flask in a magnetic constant temperature water bath. The reaction was thoroughly carried out at 45 °C for 120 minutes, then add a large amount of deionized water to terminate the reaction and remove residual sulfuric acid by vacuum filtration. This process need to repeat 2–3 times until the solution is neutral, then transfer the washed neutral solution to the dialysis bag which placed in a large beaker containing distilled water for 2 days. Finally, the NCC suspension of the dialysis bag was freeze-dried to obtain a rod-shaped nanocrystalline cellulose powder while the microcrystalline cellulose that has not been acid-decomposed will remain in the dialysis bag.

2.3. Synthesis of nanocrystalline cellulose crosslinker (NBC)

The flask was placed in a magnetic constant temperature water bath at 65 °C, and a 60 wt% composite solvent (glycerol : water = 1 : 3) was added to the flask, and then sodium hydroxide of 2 wt% was added. Stirring was continuous until the borax was completely dissolved, then 25 wt% of the ligand (glucose : glycerol = 1 : 4) was added and heated to 85 °C. The 85 °C was maintained and stirred at low speed, OBC (boric acid ester) was obtained after 4–5 hours of sufficient reaction.

The nanocellulose cross-linker is prepared by *in situ* polymerization method (Fig. 1). Briefly, 3 g of NCC and 12 g of KH550 were placed in a three-necked flask containing absolute ethanol and placed in a constant temperature water bath at 85 °C, and magnetically stirred until a homogeneous mixture was obtained. Then, 12 g of OBC was slowly added dropwise to the mixed solution, and the reaction was continued at 85 °C for

3 hours in order to the modification reaction sufficiently occurred. Then, add three times of absolute ethanol to stop the reaction, and the absolute ethanol is removed by rotary evaporation to obtain nano-crosslinker powder.

2.4. Preparation of HPG gels

Firstly, 500 g of tap water was poured into the high-speed mixer which the speed was adjusted until the liquid formed a vortex. Then, 1.5 g of HPG was slowly added and stirring was continued for 5 minutes until a 0.3 wt% HPG solution was formed. The beaker containing HPG solution was placed in a constant temperature water bath which the temperature was 30 °C standing for 4 hours until a uniformly stable HPG base liquid was obtained. Finally, pour a certain amount of HPG solution into the blender, and add different volumes of 2 wt% sodium hydroxide solution to adjust the pH value of the HPG solution from 7–14. The addition amount of NBC crosslinker ranges from 0.2 wt% to 0.9 wt%. It needs to be stopped stirring and place the formed gel for 1–2 minutes after the nano-crosslinker powder is completely dissolved, and the gel performance will show better. This is attributed to the nano-crosslinker molecules and HPG molecules are fully stretched so that they will be more closely integrated.

2.5. Characterization of NCC and NBC

TEM test was performed using a JEM-2000 transmission electron microscope (JEOL Ltd., Japan), and the prepared NCC was scanned between 400 cm^{-1} and 4000 cm^{-1} to determine its morphology and particle size distribution. NCC and NBC was ground into a powder, mixed with potassium bromide powder and compressed into flakes, and the surface modification success was verified by FTIR spectroscopy (Nexus FTIR spectrometer). XRD patterns of different samples were recorded using an X-ray diffractometer (X'Pert-APD, PANalytical, EA Almelo, The Netherlands) with an X-ray generator (3 kV) and anode (LFF Cu) at 30 mA and 40 kV. The angle used for scanning was from 10° to 60°.

2.6. Rheological measurements of HPG gels

The rheological measurements were performed with a HAAKE MARS III Rheometer System using rotor (4.2 mm gap) to measure the residual viscosity of the gel after shearing at 170 s^{-1} and 110 °C for 60 min. The gel formed by crosslinking the nano-crosslinker was freeze-dried using liquid nitrogen under a vacuum atmosphere, and then the morphology and structure of the gel were observed by a scanning electron microscope (JEOL Ltd, Japan).

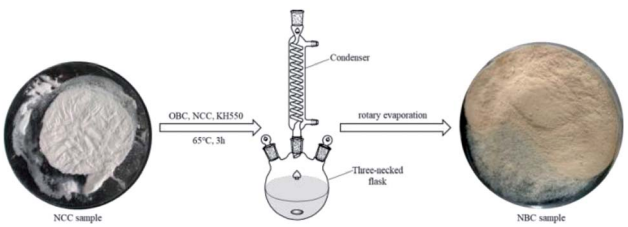

Fig. 1 The synthesis process of nano-crosslinker.

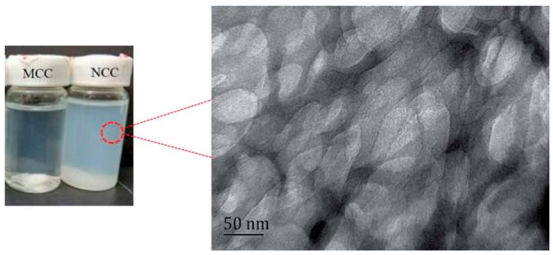

Fig. 2 Dispersion of MCC and NCC in water and TEM image of NCC.

3. Results and discussion

3.1. Characterization of NCC and NBC

Fig. 2 presented dispersion of MCC and NCC in water and TEM image of NCC. Fig. 3 shows the distribution of NCC particles in water. As shown in Fig. 2 that NCC is a rod-shaped particle with a large aspect ratio. As can be seen from Fig. 3, the average size of NCC generally between 10–30 nm in diameter and between 50–200 nm in length. Thus, NCC has a larger specific surface area, which means that the NCC surface contains more sites that are conducive to surface modification. Since the NCC is in the nanometer size range, the water dispersion of the NCC particles exhibits blue light. In addition, NCC suspension can stably dispersed in water for more than 90 d. Its due to NCC particles have anions which the introduction of sulfate groups on the surface during acid hydrolysis.

Fig. 4 presented FTIR spectra of NCC and NBC. As shown in Fig. 4, the infrared spectra of the two are roughly the same. They all have obvious characteristic peaks at 3340 cm^{-1}, 2916 cm^{-1}, 1372 cm^{-1}, 1430 cm^{-1} and 1058 cm^{-1}, which are the characteristic peaks of –OH stretching vibration of cellulose, CH stretching vibration characteristic peak, CH bending vibration characteristic peak, $-CH_2$ and –OCH in-plane bending vibration peak and COC stretching vibration peak. In addition, the characteristic absorption peaks of silane coupling agent KH550 appear at 690 cm^{-1} and 1601 cm^{-1}, which correspond to the

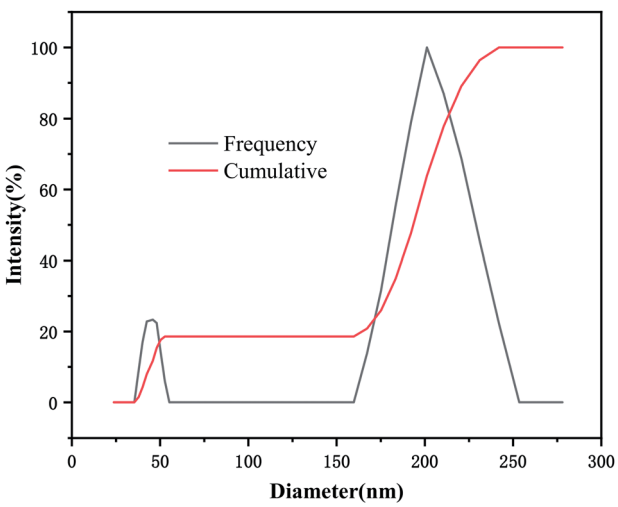

Fig. 3 Particle size distribution curve of NCC in water.

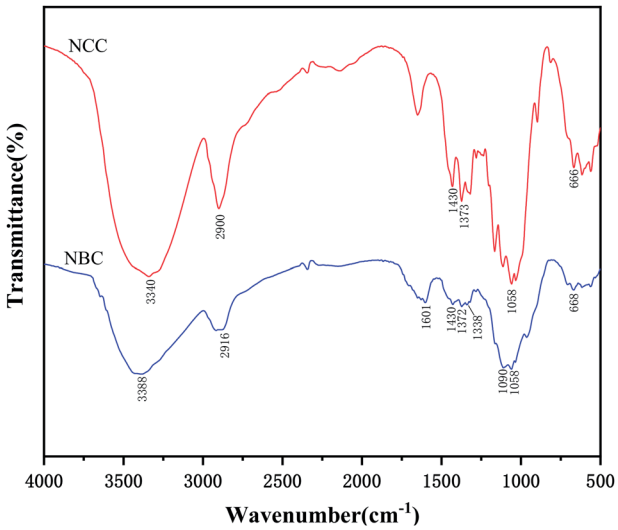

Fig. 4 FTIR spectra of NCC and NBC.

bending vibration peak of $-NH_2$ and the out-of-plane bending absorption peak of N–H, respectively. The absorption peaks at 1090 cm^{-1} and 1295 cm^{-1} correspond to the characteristic peaks of Si–O and Si–OH, respectively.[32,33] The B–O characteristic absorption peak of the NBC curve at 1338 cm^{-1} can prove that the nanocrystalline has been successfully modified, and the OBC has been successfully grafted onto the surface of the nanocrystalline cellulose.

Fig. 5 shows the XRD diffraction characterization curve of the nanocellulose before and after modification. The NCC particles prepared by sulfuric acid hydrolysis have obvious diffraction peaks at $2\theta = 14.8°$, 16°, and 22.43°, indicating that NCC is cellulose type I.[34,35] NCC particles modified by KH550 has no new diffraction peaks as well NBC crosslinker, indicating that the NCC after surface modification is still cellulose type I. It further shows that the modification of nanocellulose by KH550 only occurs on its surface without destroying the crystalline area

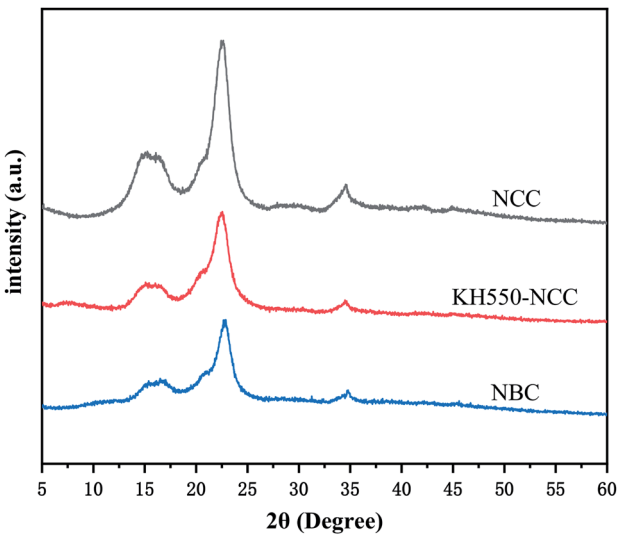

Fig. 5 XRD curve of NCC, KH550-NCC, NBC.

Fig. 6 Dispersion of NCC and NBC in guar gum solution.

inside the NCC, which is very important for the further functionalization of nanocellulose.

The NCC particles and NBC were added to the guar gum solution and fully stirred. The dispersion of NCC and NBC in the guar gum solution is shown in Fig. 6. It can be seen from Fig. 6 that the guar gum solution is divided into two layers, and the NCC particles settle to the bottom of the solution. Due to NBC and guar gum form a gel, NBC particles stably dispersed in the guar gum solution. The dispersibility of NBC in the guar gum fracturing fluid become better and the agglomeration phenomenon is weakened, due to the hydrophilicity is reduced as the number of surface hydroxyl groups is reduced after the alkylation modification of nanocellulose.

3.2. Effect of pH on rheological properties of HPG gel

The viscosity of HPG base fluid is greatly affected by pH, mainly because OH^- will affect the stretching state of HPG molecules in the solution and the formation of hydrogen bonds between them and water molecules. With the increase in pH values, the gel rigidity and gel elasticity gradually decreased while the viscous characteristics increases. At pH = 14, the guar gum chain conformation was completely coiled, which prevented the crosslinking reaction. According to the viscosity values, the pH can be divided into three areas: high viscosity area (pH = 8.5–12), medium viscosity area (pH = 7–8, pH = 12.5–13) and low viscosity area (pH = 13.5–14).[36,37]

Fig. 7 demonstrated SEM images of HPG gels. As shown in Fig. 7 that although NBC crosslinker can crosslink guar gum under neutral conditions, but the gel structure formed is not dense. The morphology of HPG gel formed by NBC at pH = 10 have the most complex and the highest viscosity and the best temperature resistance, however, the microstructure of HPG gel formed by NBC is destroyed when the pH = 14. Fig. 8 shows that

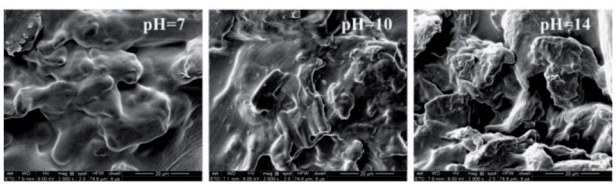

Fig. 7 Effect of pH on morphology of NBC gel.

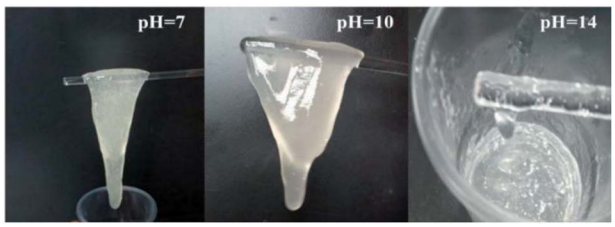

Fig. 8 Effect of pH on the hanging performance of NBC crosslinked fracturing fluid.

NBC gel can be crosslinked under neutral conditions and can be hung with glass rods. HPG gel has the best hang performance and better viscoelasticity at pH = 10, and the gel is partially dehydrated and cannot be hung when the values of pH increases to 14. The hung-up performance and microscopic morphology of HPG with pH changes can well explain the changing trend of HPG gel rheological properties in Fig. 9.

The apparent viscosity of the 0.3 wt% HPG base fluid was tested at 30 °C is 12.5 mPa s. Fig. 9 presented the residual viscosity of HPG gel after 60 min shearing at different pH values and 170 s^{-1}. The viscosity of the HPG gel formed by NBC increases first and then decreases as the pH value increasing. The remaining viscosity of the HPG gel formed by NBC at pH = 7 is greater than 72 mPa s, and the residual viscosity reaches the highest 189 mPa s at pH = 10. The remaining viscosity of the nano-crosslinked fracturing fluid gel is not much different while pH = 11 and pH = 9. In addition, the residual viscosity of the gel does not increase instead of shows a downward trend while the pH value exceeds 10. After the pH exceeds 10, the ability of HPG molecules to thicken the solution becomes poor. Due to excessive OH^- will make the grid compact and the HPG molecules are not fully stretch, thus result in the number of groups that can be combined with the crosslinker is reduced and poor crosslinking effect.

3.3. Effect of crosslinking ratio on rheological properties of HPG gel

Fig. 10 presented effect of crosslinking ratio on viscosity of HPG gel. As shown in Fig. 10, the residual viscosity of HPG gel increases rapidly when the crosslinking ratio is increased from 100 : 0.2 to 100 : 0.6. HPG gel has the highest residual viscosity when the cross-linking ratio is 100 : 0.6 and then the residual viscosity began to decrease with the cross-linking ratio continue increase.

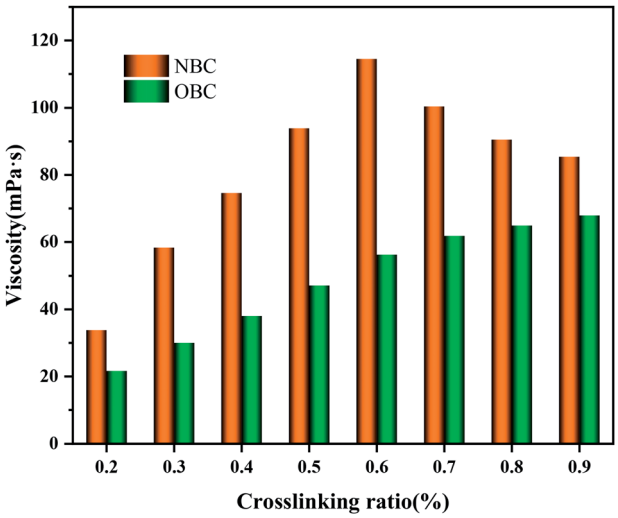

Fig. 10 Effect of crosslinking ratio on viscosity of HPG gel.

When the cross-linking ratio is low, the cross-linker can only crosslink with part of the HPG molecules, thus HPG gel has poor performance. The network structure formed by HPG gel becomes more complicated because more HPG molecules are cross-linked with the increase of crosslinker. HPG molecules have been completely cross-linked with the increase in the amount of cross-linker. The HPG gel grid will be compressed and the HPG gel will not be shear resistant due to the excess crosslinker, resulting in a smaller residual viscosity. In addition, the NBC will agglomerate as its number continues to increase, thereby affecting the cross-linking performance of the crosslinker.

Fig. 11 shows the residual viscosity of the HPG gel at 0.25 wt% HPG and 100 : 0.6. As shown in Fig. 11, the trend of HPG gels residual viscosity formed when the amount of guar

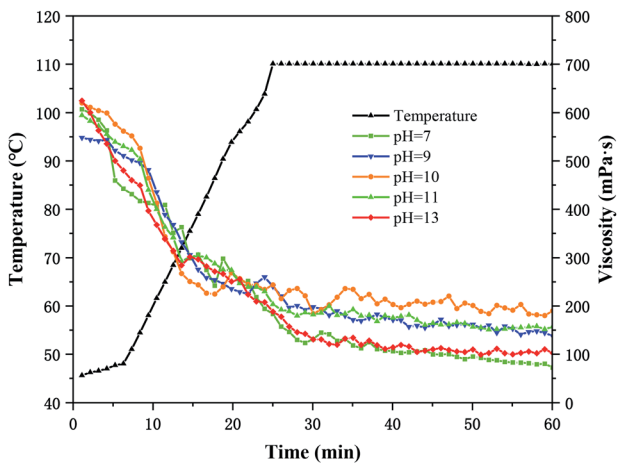

Fig. 9 Effect of pH on shear resistance of NBC crosslinked fracturing fluid.

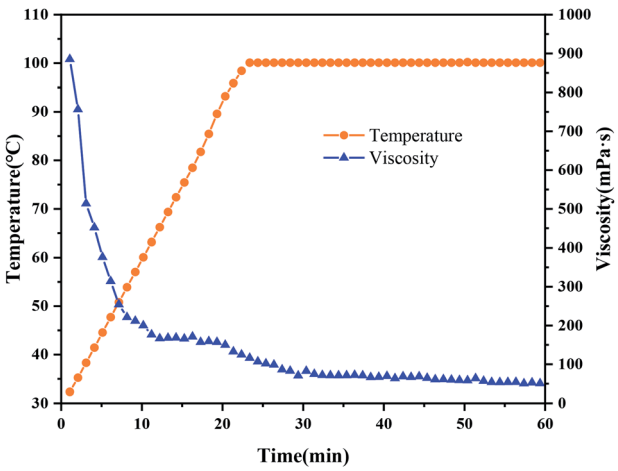

Fig. 11 Residual viscosity of 0.25 wt% HPG gel.

gum is 0.25 wt% changes with temperature and time. Due to the residual viscosity of the gel is greater than 50 mPa s after shearing at 170 s^{-1} and 100 °C for 60 minutes, thus the minimum HPG dosage of NBC crosslinker is 0.25 wt%.

3.4. Viscoelastic performance of HPG gel

The viscoelasticity of the nano-crosslinked fracturing fluid gel is expressed by the elastic moduli (G') and loss modulus (G''), and sand carrying capacity of hydraulic fracturing fluids was characterized by δ (the ratio of loss moduli to elastic moduli). It is generally thought that proppant can be sufficiently suspended in hydraulic fracturing fluids under the condition of gels presenting elastic behavior ($\delta < 1$).[38–40]

Fig. 12 presented the trends of (G') and (G'') of HPG gels with time. The nano-crosslinking fracturing fluid was prepared under the conditions of pH = 10 and the crosslinking ratio of 100 : 0.6, and the G' and G'' after 4 minutes of shearing time at a shear frequency of 1 Hz were analyzed. As shown in Fig. 12, the storage modulus of the gel is always greater than the dissipation modulus, which indicates that the nano-crosslinked fracturing fluid has good viscoelasticity. This shows that the nano-crosslinked fracturing fluid gel has good sand carrying performance.

The suspended sand experiments also demonstrated this performance of the gel. The pH value of the nano-crosslinking fracturing fluid suspended sand test was determined to be 10, and the crosslinking ratio was determined to be 100 : 0.6. The swelled 0.3 wt% guar gum solution is selected, and the proppants are all 20–40 mesh standard ceramsite. Repeat the measurement three times and take the average value. In the suspended sand test, the sedimentation rate of the 20–40 mesh ceramsite in the nano-crosslinked fracturing fluid was 0.32 cm min^{-1}.

3.5. Delayed crosslinking performance

This study shows that pH, crosslinking ratio and material ratio are the main factors affecting the crosslinking time. Table 1 shows the trend of NBC and OBC cross-linking time affected by pH. The crosslinking time of the two cross-linking fracturing fluids is proportional to the pH value and the cross-linking time of NBC is significantly longer than that of OBC. In addition, the HPG gel formed by NBC under neutral conditions can be hung with a glass rod. According to existing literature studies, the crosslinking time of the organoboron crosslinker is about 90 s. Moreover, it cannot be crosslinked to form a gel in a neutral environment.[41,42]

Table 1 Delayed crosslinking performance of NBC

pH		7	8	9	10	11	12	13	14
Crosslink time	NBC	31	52	108	122	144	176	214	227
	OBC	13	26	35	58	74	79	86	110

Only the dissolving part of the crosslinker will form cross-links with the HPG molecules while the nano-crosslinker powder is added to the HPG base liquid, and most of the crosslinker take longer to dissolve, thus prolonging the cross-linking time. In addition, as the alkalinity of the HPG base fluid increases, the rest OH^- in the solution will combine with the cross-linker molecules and HPG molecules, which will also increase the cross-linking time.

The experiments in this paper show that the crosslinking time decreases with the increase of the crosslinking ratio. The decrease in cross-linking time is attributed to the increase in cross-linking sites as the cross-linking ratio increases, which results in more HPG molecules that can be cross-linked at the beginning of the cross-linking reaction. In addition, when the pH value of the base fluid is constant, the performance of the gel is improved as the crosslinking ratio increases. When the material ratio (NCC : OBC) increased from 1 : 2 to 1 : 5, the crosslinking time increased significantly. Due to the modification efficiency and performance of NBC prepared becomes higher with the increase of OBC when the amount of NCC is kept constant, thus the performance of delaying crosslinking time is enhanced. Most of the NCC particles have been surface modified when the material ratio (NCC : OBC) reaches 1 : 6. There are few NCC particles that can be modified with the amount of OBC increasing, thus the performance of the prepared NBC is not improved significantly and the delayed crosslinking performance of NBC reaches its optimum at this time. The crosslinking time can be controlled by controlling the added amount of crosslinker and the pH of the HPG base fluid when the material ratio (NCC : OBC) is 1 : 6 to prepare NBC.

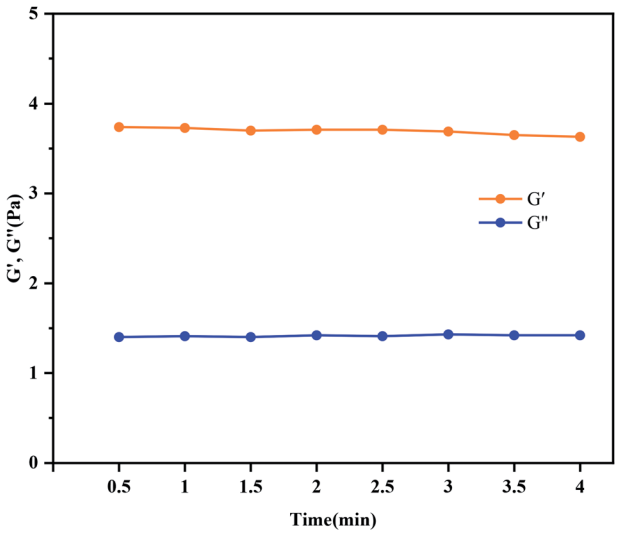

Fig. 12 Viscoelastic performance of HPG gel.

3.6. Temperature resistance performance

Fig. 13 shows the temperature resistance of NBC and OBC under the conditions of optimal pH and crosslinking ratio. The residual viscosity of the gel exhibits a trend as the temperature rises uniformly of first decreasing rapidly and then slowly decreasing. The residual viscosity of the gel drops below 100 mPa s while the temperature increases to 150 °C, but when the temperature increases above 160 °C, the residual viscosity of the gel drops below 50 mPa s. This indicates that the temperature resistance of HPG gel formed by NBC reaches 160 °C. Due to the

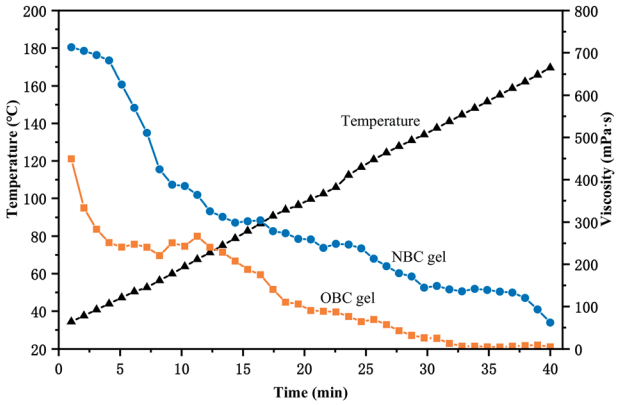

Fig. 13 Temperature resistance of NBC crosslinked fracturing fluid.

large number of hydrogen bonds formed during the cross-linking process of polymers, NBC greatly improve the temperature resistance of guar gum fracturing fluid compared with OBC. Therefore, the rheological evaluation of guar gum fracturing fluid is carried out at 110 °C, which is 10 °C higher than other types of nano-crosslinker.

3.7. The durability of the NBC gels with respect to salinity

Most of the water contained in oil reservoirs is the mineralization of water which has a high salt content. Therefore, the salt tolerance of fracturing fluid is an important indicator to measure its performance.

We used KCl to prepare solutions with different salinities and studied the salt resistance of nano-crosslinked fracturing fluids. The experimental results are shown in Fig. 14. It can be seen from Fig. 14 that the viscosity of the organoboron cross-linked fracturing fluid decreases rapidly with the increase of the salt content. The viscosity of nano-crosslinked fracturing fluid can remain stable with the increase of KCl content at the beginning. When the KCl mass fraction increased to 1.5 wt%, the viscosity of the nano-crosslinked fracturing fluid began to decrease. The viscosity of nano-crosslinked fracturing fluids was always higher than that of the organic boron cross-linked fracturing fluid.

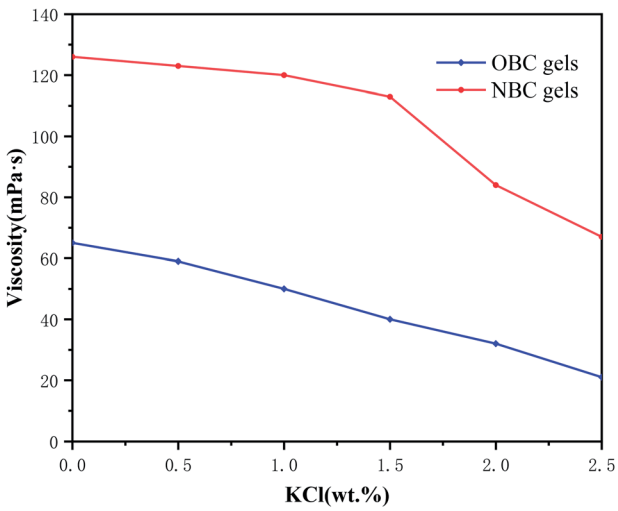

Fig. 14 Salt resistance of nano-crosslinked fracturing fluid.

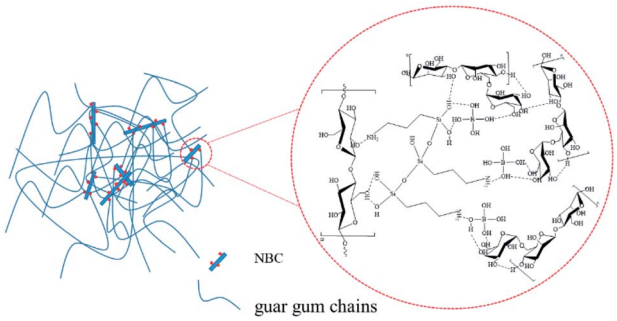

Fig. 15 Network structures of NBC crosslinked HPG.

3.8. Mechanism of NBC crosslinking HPG

Fig. 15 shows the principle diagram of NBC cross-linking HPG. It can be seen from Fig. 15 that the silane coupling agent KH550 combines NCC through the formation of a hydrogen bond between the hydroxyl group while the other end of the silane coupling agent combines with the organoboron through the amino group ($-NH_2$) to form a B–N bond. Similarly, another connection method is to combine the amino end ($-NH_2$) of the silane coupling agent KH550 with nanocellulose particles. The other end through the hydroxyl group to bind organoboron to form a B–N bond. A variety of combinations make the network structure formed by the nano-crosslinker more complicated, so the gel formed has better performance. During the cross-linking process, each nanocrystalline cellulose molecule can be grafted with multiple OBC molecules through a silane coupling agent to form multiple branches, and the nanocrystalline cellulose particles are used as the skeleton to crosslink the guar gum molecules through multiple branch chains to form a complex network structure. Existing studies have proved that the hydroxyl groups on the surface of organoboron and the homeopathic hydroxyl groups of guar gum molecules combine to form hydrogen bonds. The combination of NBC and HPG will form a complex network structure that was combined through the formation of hydrogen bonds.[43,44]

Besides, the surface of nano-cellulose molecules contains a large number of active hydroxyl groups, which may form hydrogen bonds between them. Therefore, the nano-crosslinker itself has a thickening effect on the aqueous solution. The spatial size of nano-cellulose crosslinker and the existing crosslinking sites have been greatly increased compared with OBC, which is beneficial to crosslinking guar gum molecules. Therefore, NBC has a higher crosslinking efficiency and the resulting gel has excellent performance.

4. Conclusion

Nanocellulose was prepared by acid hydrolysis and used to prepare a novel nanoboron crosslinker. NBC is prepared by

surface modification of NCC using KH550 and OBC. The modification of NCC with KH550 only takes place on the surface and does not damage the internal structure of nanocellulose thus the modified nanocellulose is still type I.

The delayed crosslinking performance of NBC is better than that of OBC. NBC can crosslink HPG to form HPG gels that can be hung-up by glass rod under neutral conditions. The residual viscosity meets the experimental requirements under shear at 170 s^{-1} and 110 °C for 60 minutes when the pH increases from 7 to 13. The HPG gel formed by NBC crosslinking can withstand a temperature of 160 °C and crosslinked 0.25 wt% HPG fracturing fluid under this condition of pH = 10 and 100 : 0.6 of crosslinking ratio. Nano crosslinker has better crosslinking efficiency and salt resistance performance compared with ordinary organic boron crosslinkers. Nano-crosslinker is bonded together through the formation of hydrogen bonds between the organoboron and HPG molecules grafted on the surface. NCC exists as a skeleton in the HPG gel formed by NBC cross-linking. It has more cross-linking sites and better cross-linking performance due to its larger aspect ratio.

Conflicts of interest

There is no conflict to declare.

Acknowledgements

Financial support by the Joint Funds of the National Natural Science Foundation of China (U1762212) is gratefully acknowledged. The funders had no conflict of interest or any role in the study design, data collection and analysis, decision to publish or preparation of the manuscript.

References

1 R. Barati and J. T. Liang, *J. Appl. Polym. Sci.*, 2014, 131.
2 J. Z. Zhao, S. H. Li, X. F. Qu and L. L. Liu, *Pet. Explor. Dev.*, 2002, **29**, 93–95.
3 L. Li, G. A. Al-Muntasheri and F. Liang, *Petroleum*, 2016, **2**, 313–323.
4 G. Al-Muntasheri, *Society of Petroleum Engineers Western North America and Rocky Mountain Joint Conference and Exhibition 2014*, 2014, vol. 2.
5 Y. Cheng, K. M. Brown and R. K. Prud'homme, *Biomacromolecules*, 2002, **3**, 456–461.
6 S. Kesavan and R. K. Prud'homme, *Macromolecules*, 1992, **25**, 2026–2032.
7 R. Lapasin, L. De Lorenzi, S. Pricl and G. Torriano, *Carbohydr. Polym.*, 1995, **28**, 195–202.
8 R. Moorhouse, D. N. Harry, L. Matthews and U. Merchant, *presented in part at the SPE India Oil and Gas Conference and Exhibition*, New Delhi, India, 1998/1/1.
9 N. J. Williams, P. A. Kelly, K. G. Berard, E. L. Dore, N. L. Emery, C. F. Williams and S. Mukhopadhyay, *presented in part at the SPE International Symposium and Exhibition on Formation Damage Control*, Lafayette, Louisiana, USA, 2012/1/1.
10 X. Lin, P. Tang, C. Zheng, *et al.*, *J. Adv. Phys. Chem.*, 2017, **06**, 37–43.
11 M. Legemah, M. Guerin, H. Sun and Q. Qu, *SPE J.*, 2014, **19**, 737–743.
12 B. Xiao, S. Zhang, J. Zhang, T. Hou and T. Guo, *Physicochem. Probl. Miner. Process.*, 2015, **51**, 37–47.
13 M. Bishop, N. Shahid, J. Yang and A. R. Barron, *Dalton Trans.*, 2004, 2621–2634, DOI: 10.1039/B406952H.
14 J. Kramer, R. K. Prud'homme, P. Wiltzius, P. Mirau and S. Knoll, *Colloid Polym. Sci.*, 1988, **266**, 145–155.
15 J. Liu, S. Wang, C. Wang, F. Zhao, S. Lei, H. Yi and J. Guo, *Carbohydr. Polym.*, 2020, **234**, 115915.
16 V. Lafitte, G. J. Tustin, B. Drochon and M. D. Parris, *presented in part at the SPE International Oilfield Nanotechnology Conference and Exhibition*, Noordwijk, The Netherlands, 2012/1/1.
17 K. Wang, Y. Wang, J. Ren and C. Dai, *presented in part at the SPE/IATMI Asia Pacific Oil & Gas Conference and Exhibition*, Jakarta, Indonesia, 2017/10/17.
18 T. T. Wang, Z. C. Shen and M. H. Liu, *Acta Polym. Sin.*, 2017, (1), 50–62.
19 L. Mayol, M. Biondi and F. Quaglia, *Biomacromolecules*, 2011, **12**(1), 28–33.
20 J. P. Rothstein and H. Mohammadigoushki, *J. Non-Newtonian Fluid Mech.*, 2020, **285**, 104382.
21 Y. Jiang, *Curr. Opin. Colloid Interface Sci.*, 2002, **7**(5–6), 276–281.
22 P. Phanthong, P. Reubroycharoen, X. Hao, G. Xu, A. Abudula and G. Guan, *Carbon Resour. Convers.*, 2018, **1**, 32–43.
23 A. Dufresne, *Nanocellulose: from nature to high performance tailored materials*, De Gruyter, 2012.
24 C. Salas, T. Nypelö, C. Rodriguez-Abreu, C. Carrillo and O. J. Rojas, *Curr. Opin. Colloid Interface Sci.*, 2014, **19**, 383–396.
25 J. Li, X. Wei, Q. Wang, J. Chen, G. Chang, L. Kong, J. Su and Y. Liu, *Carbohydr. Polym.*, 2012, **90**, 1609–1613.
26 Y. Tang, S. Yang, N. Zhang and J. Zhang, *Cellulose*, 2014, **21**, 335–346.
27 P. Chen, H. Yu, Y. Liu, W. Chen, X. Wang and M. Ouyang, *Cellulose*, 2013, **20**, 149–157.
28 M. Zaman, H. Xiao, F. Chibante and Y. Ni, *Carbohydr. Polym.*, 2012, **89**, 163–170.
29 L. K. Kian, M. Jawaid, H. Ariffin and Z. Karim, *Int. J. Biol. Macromol.*, 2018, **114**, 54–63.
30 S. Kalia, S. Boufi, A. Celli and S. Kango, *Colloid Polym. Sci.*, 2014, **292**, 5–31.
31 S. Mohapatra, N. Panda and P. Pramanik, *Mater. Sci. Eng., C*, 2009, **29**, 2254–2260.
32 S. Zhang, C. Xia, Y. Dong, Y. Yan, J. Li, S. Q. Shi and L. Cai, *Ind. Crops Prod.*, 2016, **80**, 207–213.
33 L. Wei, U. P. Agarwal, K. C. Hirth, L. M. Matuana, R. C. Sabo and N. M. Stark, *Carbohydr. Polym.*, 2017, **169**, 108–116.
34 J. Guo, W. Du, S. Wang, Y. Yin and Y. Gao, *Carbohydr. Polym.*, 2017, **157**, 79–85.
35 Y. Habibi, L. A. Lucia and O. J. Rojas, *Chem. Rev.*, 2010, **110**, 3479–3500.
36 P. C. Harris, *J. Pet. Technol.*, 1993, **45**, 264–269.

37 S. Wang, H. Tang, J. Guo and K. Wang, *Carbohydr. Polym.*, 2016, **147**, 455–463.
38 A. Tayal, V. B. Pai and S. A. Khan, *Macromolecules*, 1999, **32**(17), 5567–5574.
39 S. R. Raghavan and S. A. Khan, *J. Colloid Interface Sci.*, 1997, **185**, 57.
40 S. Kesavan and R. K. Prud'Homme, *Macromolecules*, 1992, **25**(7), 2026–2032.
41 N. Shao, Y. S. Yan and P. H. Yu, *Oilfield Chem.*, 2019, **36**(3), 388–393.
42 H. Bai, J. Zhao and P. Tian, *Fine Chem.*, 2015, **32**(10), 1157–1161.
43 X. Ke, G. Baoshan, X. Minjie, L. Ping and W. Haiyan, *IOP Conf. Ser.: Mater. Sci. Eng.*, 2018, 423.
44 T. Hurnaus and J. Plank, *Energy Fuels*, 2015, **29**, 3601–3608.